Thermal Analysis and Fatigue Verification of the LWR for an Effective Maintenance of the Railway Transport Network

Michele Agostinacchio
Full Professor of Roads, Railways and Airports
University of Basilicata - Italy
agostinacchio@unibas.it

Donato Ciampa
PhD Student
University of Basilicata – Italy
ciampa@unibas.it

Synopsis

The increase in trains velocity and the improvement of comfort on railways belong to both the improvement of vehicles performances and to the use of the long welded rail (LWR).
The analysis of the thermal set-up of the track is fundamental for the sake of the railway transport network performances: it basically deals with the changes in spans and strains occurring daily after temperature ranges. This phenomenon is described by the free dilatation law for tracks without bonds and by the stopped dilatation law for completely constrained tracks.
The thermal analysis of the LWR shows a cyclic soliciting phenomenon belonging to both the daily temperature ranges and to the effects of moving vehicles: from this point of view a repetition of strains which involves an appropriate fatigue verification of the railways can be identified.
For this reason the authors propose a procedure based on the synergic application of the Woehler construction theory for the fatigue curves and of the Miner law of linear accumulation.
Once the Woehler curves are found as function of the different stress state due to the thermal variations and to the moving vehicles passing, the comprehensive damage for both kinds of strains can be quantified by means of the Miner theory.
For this purpose the authors propose the implementation of a calculation software which can automate the thermal lay-out analysis phase, performing the Woehler curve, the internal stresses computation and the damage analysis following Miner's law.
In conclusion, this research is an useful tool for an effective maintenance of the LWR, as it allows the monitoring of the stress state of tracks, especially during the last part of their life cycle, when the temperature range and the moving vehicles passage consequences are more severe.

Thermal Analysis and Fatigue Verification of the LWR for an Effective Maintenance of the Railway Transport Network

The long welded rail, commonly called LWR is a rail without joints, obtained by welding fixed length rails and with two common joints at the edges.
The central part of the element (body), differently from the traditional railing with joints, is not subjected to any sliding due to the daily thermal temperature differences.
The following advantages derive from the use of the so-called LWR:

- reduction of maintenance, because of the limited number of traditional joints;
- increased running speed of trains;
- improved ride comfort;

At the same time, a higher attention is required during controls in order to avoid anomalous situations from the point of view of stresses and strains of the track
Starting from this idea, the Authors decided to deepen the study of the thermal set-up of the LWR along with the fatigue phenomenon due to thermal variations and to the repeated passage of moving loads, proposing an automatic solution of the problem, by means of a code calculation arranged for the purpose.

FREE DILATION AND PREVENTED DILATION OF THE RAIL

Because of temperature differences due to climate the rail is subjected to length variations and/or to stress state variations. The law which describes the phenomenon is, in the case of rail free from bonds, the law of free dilation, which is:

$$\Delta l = \alpha \cdot l \cdot \Delta t \quad (1)$$

with the following meaning of the symbols:

- Δl = length variation of the rail;
- α = steel linear dilation coefficient, equal to 0.0000115°C^{-1};
- l = initial length of the rail;
- Δt = temperature variation in °C.

In case of completely bond track the prevented dilation law is applied, which includes that a compressive or tensile thermal force F corresponds to a thermal variation ΔT, which is equal to:

$$F = \alpha \cdot E \cdot A \cdot \Delta t \quad (2)$$

where:

- E = longitudinal elasticity modulus equal to 20601000N/cm^2;
- A = transversal section of the rail in cm^2.

Since the values of α and E are fixed , the equation (2) can be re-written in the following way:

$$F = 237 \cdot A \cdot \Delta t \quad (3)$$

to which corresponds a thermal tension σ in N/cm^2 equal to:

$$\sigma = 237 \cdot \Delta t \quad (4)$$

The following oppose to the free dilation of the rail:

1) friction resistance of junctions;
2) friction resistance of supports.

In particular this dilation is blocked by the following factors:

- direct contact with heads, when the dilation causes the closure of clearances;
- junction organs when, after shortening the maximum clearance is reached, fixed from Ferrovie dello Stato in 14mm.

FRICTION RESISTANCE OF JUNCTIONS

The junction organs oppose to sliding of heads through friction forces inducted by the fastening of the screws of the joggles.
These forces depend on different factors (length of the fastening key, operator applied force, contact surface characteristics, etc.), therefore their evaluation is very complex. Because of these considerations [2] assume as limiting friction resistance of the junctions a concentrated force R_g equal to 58.86kN (60t), equal to the

force obtained fastening the joggles with a 38cm long key, used by a unique man after lubrication of the contact surfaces with oil and graphite mixed together. The reaction R_g acts in the direction opposed to the movement of the head.
It is defined thermal change T_g (°C) necessary to overtake the friction resistance of the junctions, the variation of temperature needed to generate in the rail a thermal force which overtakes the friction resistance of the junctions. The thermal change T_g is obtained imposing that the thermal force (Cfr. Eq. 3) and the friction resistance R_g are equal, which implies:

$$Tg = \frac{R_g}{237 \cdot A} \tag{5}$$

with:
- R_g = junction resistance in N;
- A = transversal section of rails in cm^2.

SUPPORTS RESISTANCE

This resistance is composed by two aliquots: the bindings resistance and the resistance of the ballast.
The first is due to the friction resistance between the sole and the plate and depends on the contact pressure and to the friction coefficient (generally [16] is assumed equal to 7.5kN for an indirect or elastic binding).
The ballast resistance expressed by the force r_m explicates, indeed, through sleepers and ballast.
Also this resistance is influenced by several factors, and its calculation is very difficult, so it is assumed as a uniformly distributed force along the rail [2], equal to:
- 8.8 kN for pre-stressed concrete sleepers rails in a tenacious gravel with regular particle size with indirect and elastic bindings;
- 5.9 kN for tracks made of wooden sleepers in a tenacious gravel with regular particle size with indirect and elastic bindings.

The thermal change T_m (°C) is defined as the temperature variation needed to start a thermal force which can overtake the overall resistance of the ballast (started cycle phase). The thermal change T_m is obtained imposing the identity between the thermal force (Cfr Eq. 3) and the overall resistance which is measured in the centre line of the rail, or [2]:

$$r_m \cdot \frac{L}{2} = 237 \cdot A \cdot T_m \tag{6}$$

from which:

$$T_m = \frac{r_m \cdot L}{2 \cdot 237 \cdot A} \tag{7}$$

with the following symbols meaning:
- r_m= unitary resistance of the ballast in kN/m;
- L= length of the rail (in cm);
- A= transversal section of the rail in cm^2.

DEFINITION OF LONG WELDED RAIL

The FS instructions n°2 datated 19/11/1990 [11] based on the " Instructions for the construction and control of the LWR" gives the following definitions:
- "*track of the long welded rail (LWR) is that track in which the rails dilations (contractions) due to thermal changes cannot happen at the end of the rails, a central part being still when the temperatures of the rails themselves change: the temperature variations generate, indeed, in this central part, only a variation of the longitudinal stresses in the rails (internal stresses) proportional to the just mentioned temperature variations*";
- "*continuous track is that arranged, levelled and ranged and made of rails progressively welded, without interruptions for lengths longer than 144 metres, waiting for regulation*";
- "*average temperature t_m (°C) the arithmetic mean between the maximum temperature and the minimum one of rail, according to the climatic local conditions*:

$$t_m = \frac{t_{\max} + t_{\min}}{2} \tag{8}$$

where t_{max} and t_{min} are respectively the mean values of the maximum temperatures and the mean value of the minimum temperatures measured, also in different places of the same track, in a period of at least 3 years";
- "*laying temperature t_p (°C) the effective temperature of the rail measured at the moment of the fastening of the binding organs*";

– "*regulation temperature t_r (°C) or neutral, that temperature for which the LWR is free from internal stresses; it is assumed to be equal to the mean temperature t_m increased by 5 °C*".

BEHAVIOUR OF THE EDGES OF THE LWR

The clearances diagram interesting the mobile edge of the LWR is represented in Fig.1. The starting point is the regulation of the continuous track highlighted by a temperature t_r and a void clearance.
As the temperature decreases there is a first part of prevented dilation, during which the junctions resistance stops every sort of movement of the head (vertical segment). The rail starts moving after a thermal excursion T_g (Cfr. Eq. 5).
After the resistance of the joining organs is overtaken, a thermal change T_1 is necessary to win the ballast resistance which is equal to:

$$T_1 = \sqrt{k \cdot g} \tag{9}$$

with the following symbols meaning:

– k = $\frac{r_m}{\alpha^2 \cdot E \cdot A}$ = parabola parameter;
– g = maximum clearance allowed by the junction organs equal to 14mm;

This phase of partially prevented dilation is represented by a parabolic arc with a parameter k which increases the clearance of the void value to the maximum value of 14mm in correspondence of the opening temperature of the clearances t_a.

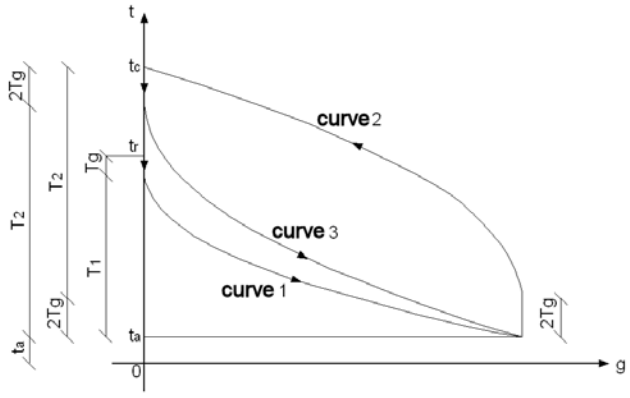

Figure 1: Diagram interesting the mobile edge of the LWR

A further decrease of the temperature does not produce any effect on the clearance. Starting from the temperature t_a an increase of $2T_g$ in the temperature is necessary to win the junctions resistance because firstly it is necessary to cancel the compression stress present in the rail, produced by an excursion T_g and then create a tensile state with a high temperature change T_g. The clearance is constantly equal to 14mm and the diagram translates into a vertical segment of $2T_g$. After a further increase of the temperature it is observed the overtaking phase of the ballast resistance, whose amplitude is:

$$T_2 = \sqrt{k' \cdot g} = \sqrt{2 \cdot k \cdot g} \tag{10}$$

up to the closure temperature of the clearances t_c. This phase is represented by a parabolic arc with parameter k' which is twice as the same value of the initial phase.
In order to complete the cycle, it is necessary to have a further phase with decreasing temperature from the value t_c to the value t_a, represented by a vertical segment equal to $2T_g$ relative to the phase of overtaking of the junctions resistance and by a parabolic arc with projection on the y axes equal to T_2 and parameter k' twice as the parameter of the starting phase of the cycle.
The limiting hysteresis cycle of the clearances of the edges for complete temperature variations is made of just mentioned parabolic arcs with parameter k'=2k and by the vertical parts which connects them.
Tracking the diagram of the stresses of the edges of the LWR it is necessary to analyse the alternation of the following phases (Cfr. Fig. 2):

– prevented dilation due to an increase of temperature from t_r to t_{max} where the thermal force changes from the void value to F_1 which is equal to:
– $F_1 = 237 \cdot A \cdot (t_{\max} - t_r)$

(11)

- prevented dilation due to a further decrease of the temperature t_{max} to t_r, where the force moves from the value F_1 to zero;
- prevented dilation due to the junctions resistance for temperature changing from t_r to (t_r–t_g), with a tensile stress increasing from zero to F_g, coming from:
- $$F_g = 237 \cdot A \cdot T_g \quad (12)$$
- partially prevented dilation between the temperature (t_r–T_g) and the temperature of clearances opening t_a, where there is a gradual opening of the clearances while the tensile stress is still equal to F_g;
- completely prevented dilation because of the complete opening of clearances in presence of temperature decreases up to the minimum value t_{min}, in correspondence of which the tensile stress reaches the maximum value F_4, equal to:
- $$F_4 = 237 \cdot A \cdot (t_r - t_{\min} - T_1) \quad (13)$$
- If the temperature increases further up to the temperature of the clearances opening the tensile stress will reduce and assume in correspondence of t_a the value F_g. This phase continues until an increase of the temperature of $2T_g$ cancels the tensile stress to transform it in an equivalent compressive stress F_g;
- partially prevented dilation between the temperature (t_a+$2T_g$) and the temperature t_c, characterised by the overtake of the ballast resistance and by a constant value of the compressive stress equal to F_g;
- completely prevented dilation by the complete closure of clearances, which involves, for a temperature increase up to t_{max}, an increase of the stress up to to value F_3, equal to:
- $$F_3 = 237 \cdot A \cdot (t_{\max} - t_c + T_g) \quad (14)$$
- If the temperature decreases up to the value t_c the compression reduces until it is cancelled and then it changes again into traction in correspondence of temperature (t_c–$2T_g$), assuming the value F_g;
- partially prevented dilation individuated between the temperatures (t_c–$2T_g$) and t_a where the ballast resistance is overtaken and the stress is constantly equal to F_g.

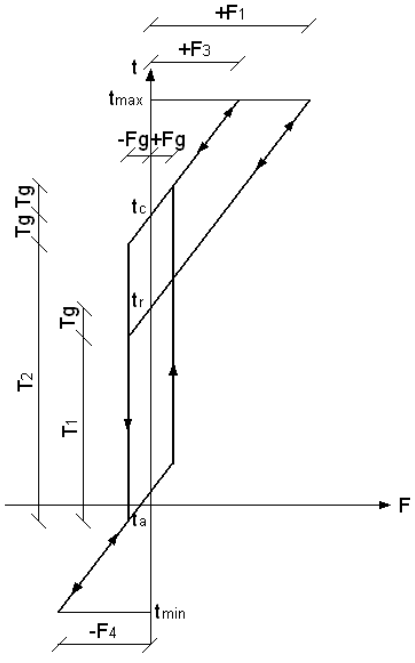

Figure 2: Diagram of the stresses of the edges of the LWR

BEHAVIOUR OF THE BODY OF THE LWR

The body of the LWR is defined as the fixed part of the rail which because of thermal variations is involved only in variations of the internal stress state. The diagram of the forces corresponding to the fixed part of a LWR as function of the temperature t (Cfr. Fig. 3) is represented by a line passing through the y value t_r whose equation is:

$$F_1 = 237 \cdot A \cdot (t - t_r) \tag{15}$$

This line is covered in both directions between the maximum tensile value in correspondence of the temperature t_{min}:

$$F_{traction} = 237 \cdot A \cdot (t_{\min} - t_r) \tag{16}$$

and the maximum compressive value in correspondence of the temperature t_{max}:

$$F_{compression} = 237 \cdot A \cdot (t_{\max} - t_r) \tag{17}$$

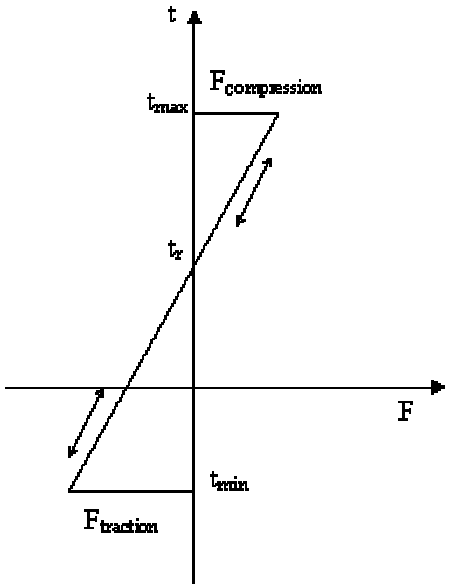

Figure 3: Diagram of the forces corresponding to the fixed part of a LWR

OUTILINES OF THE FATIGUE THEORY

Steel structural elements during their life can be subjected to stresses changing with time in a cyclical manner, thus to loads where it is possible to identify a series of tensile values which alternates from a minimum value to a maximum one.

These elements are damaged after the just mentioned tensions even though the maximum values are generally under those of rupture: in this case the fatigue rupture happens.

Fatigue is a very complex phenomenon since it simultaneously depends upon the alternated tension level and on the defects distributions located in the material and its study can be conducted, generally, through three different approaches:

- based on the nominal stress acting on the investigated section (corrected with appropriate coefficients), supposing the material has an elastic-linear behaviour;
- based on the strain, or on the localised plastic deformations during the load cycles;
- based on fracture mechanics.

The Authors referred to the first criterion in this study, because of its higher capacity in interpreting the investigated phenomenon.

WOEHLER CURVE AND FATIGUE RESISTANCE LIMIT

At the beginning of the 20^{th} century a German railway engineer, August Woehler, conducted the first systematic experiments on the fatigue phenomenon to investigate on some apparently weird rupture in work of some rails.

For this purpose he did some tests on the material changing the load in a cyclical manner with time from a fixed maximum value to a fixed minimum one.

The specimens where standardised opportunely (circular section with a diameter equal to 7.5mm with an excellent superficial finish) and subjected to pure rotating flexure with the Moore machine (Cfr. Fig. 4).

In the specific it was applied a load story with amplitude σ_a constant, the number of cycles N for rupture were registered and the results were reported in a cartesian diagram σ-N deriving in this way the so-called "Woehler curve", limited superiorly by the value σ_R corresponding to the static rupture load.

In the experimental curve of Woehler there are three different fields:

- quasi-static resistance field for $N<10^3$;
- ended fatigue field for $10^3<N<10^6$, where the equation of the curve is of this type:

$$\sigma_f \cdot N_f^{1/m} = K^{1/m} \tag{18}$$

  with m and K constants relative to the material;
- infinite resistance field, generally for $N> 10^6$, represented by a curve parallel to the axes N or with a minor slope;

For some materials, as steel there is a characteristic value $\sigma_{a\infty}$ called fatigue limit, under which the specimen can be stressed an infinite number of times, without causing any failure.

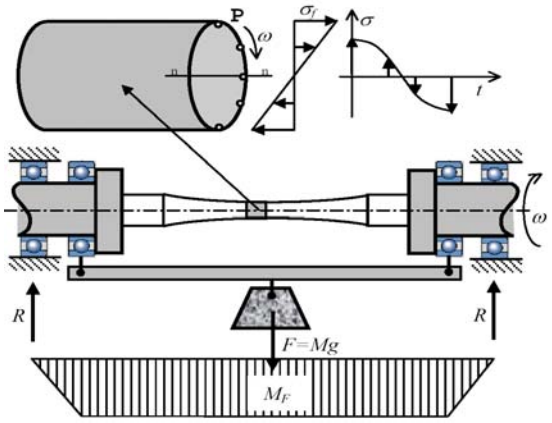

Figure 4: Schematic representation of Moore device, of the specimen and the flexure diagram. Behaviour of the tension in the point P as function of time

According to the UNI 7670 Standards for steels, without experimental data it is assumed that the higher limit σ_R is reached for a number of cycles of 10^3, while the fatigue limit $\sigma_{a\infty}$ for a number of cycles equal to $2\cdot10^6$ [17] (Cfr. Fig. 5).

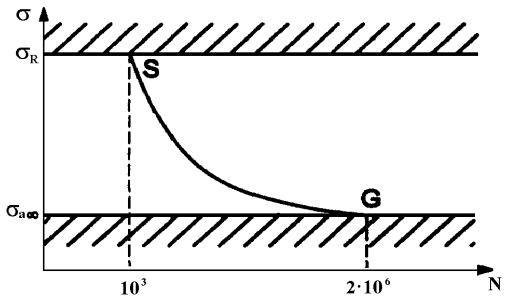

Figure 5: Curvilinear part of the Woehler diagram

The diagram presents respectively a first horizontal part, a curvilinear part SG and a final horizontal part; in order to give it more readable the bi-logarithmic representation [17] is used (Cfr. Fig. 6).

In order to determinate the equation of the inclined part it is possible to refer to the scheme of Fig. 7 [17] where σ_A and N_a represent the coordinates of a known point A and σ_a and N the coordinates of a generic point T.
Supposing the inclination angle α of the segment is known, it derives:

$$a \cdot tg\alpha = a \cdot k = b \tag{19}$$

where, considering the logarithmic coordinates:

$$k \cdot \log \frac{\sigma_a}{\sigma_A} = \log \frac{N_A}{N} \tag{20}$$

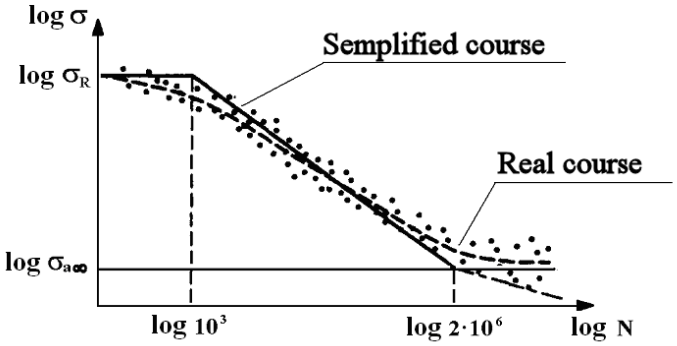

Figure 6: Bi-logaritmic representation of the Woehler diagram for AISI 1010 steel

For this reason the equation of the segment can be expressed by the following equation:

$$\frac{N_A}{N} = \left(\frac{\sigma_a}{\sigma_A} \right)^k \tag{21}$$

where:

- (σ_a, N) = coordinates of a generic point belonging to the segment;
- (σ_A, N_A) = coordinates of a known point A belonging to the segment;
- K = 8÷10 for smooth specimens;
- k = 3 ÷4 for indented specimens.

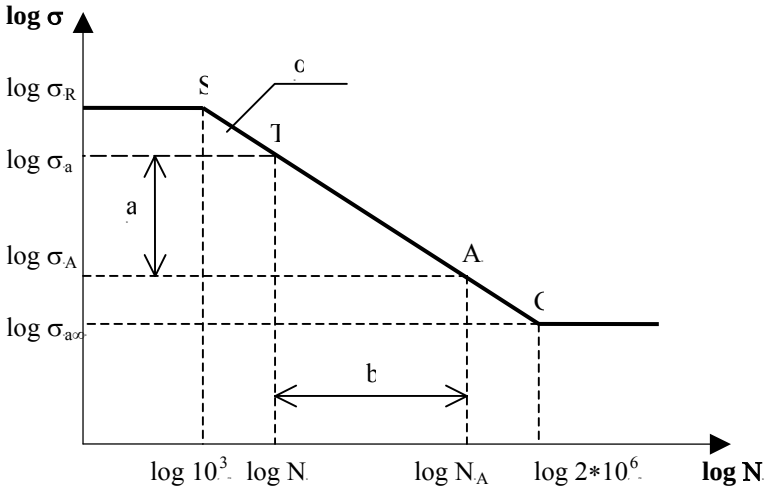

Figure 7: Sketch of the Woehler diagram in the bi-logaritmic plane

In case of rotating flexure, the fatigue rupture happens in the weakest point of the surface, while in alternated flexure, when the load changes the sign, the weakest point is not, generally, located in correspondence of the most stressed fibres.
This implies that the fatigue resistance after alternated flexure is generally higher than the corresponding one for rotating flexure.
Actually axial trials give fatigue limits equal to 90% of those obtained after rotating flexure. Moreover, in case of the present of a slight eccentricity of the load with respect to the axle of the specimen, there is a flexural stress which produces tensions slightly higher than the ratio between the applied load P and the transversal section A. In this case the effect is considered evaluating the tension produced by the sole axial stress and reducing the fatigue limit for rotating flexure of a quantity between to 20 and 30%.

Considering that this reduction is connected with differences in the stress gradient, it is included in the computation multiplying the fatigue limit $\sigma_{a\infty}$ for a gradient factor or a constant of gradient, k_c, which assumes the values included in table 1.
From the investigations carried on it was found that different factors influence the fatigue resistance for a high number of cycles and the main ones are the following:

- factors connected with the load application;
- factors connected with the resistance and the state of the material;
- factors connected with the geometry of the element.

Tab. 1: K_c values as function of the type of stress

Type of stress	k_c
Axial ($\sigma_r \leq 1520$ MPa)	0.850
Axial ($\sigma_r > 1520$ MPa)	1.0
Alternated flexure	1.0
Torsion/shear ductil materials	0.5÷0.6
Torsion/shear fragile materials	0.8÷1.0

In order to take into account all the se factors, the fatigue limit σ_f of the element studied is obtained applying the following expression:

$$\sigma_f = k_a \cdot k_b \cdot k_c \cdot k_f \cdot k_e \cdot \sigma_{a\infty} \qquad (22)$$

where the coefficients are, respectively, referred to :

- superficial finish (k_a);
- dimensions (k_b);
- gradient and type of stress (k_c);
- sensitivity to indents (k_f);
- temperature and external environment (k_e).

The coefficient k_a takes into account the superficial conditions of the element analysed by the following formula:

$$k_a = a \cdot \sigma_R^b \qquad (23)$$

where:

- σ_R = rupture tension of the material in N/mm^2;
- a,b = tabled constants (Cfr. Tab. 2) as function of the superficial finishing.

Tab. 2: Coefficients for the k_a calculation as function of the superficial finishing

Superficial finishing	a	b
Rectified	1.58	-0.085
Machine tool	4.51	-0.265
Hot laminated	57.7	-0.718
Crude	272.0	-0.995

The coefficient k_b is tabled as function of the type of stress and in particular, for rotating flexure and torsion, the values of Tab. 3 are obtained:

Tab. 3: k_b values as function of the specimen diameter

Specimen diameter (mm)	k_b
d < 10	$(d/7.62)^{-0.1133}$
10 ≤ d ≤ 50	$(d/7.62)^{-0.1133}$
50 ≤ d ≤ 100	0.6÷0.75
100 ≤ d ≤ 150	0.6÷0.75

For non circular elements and/or not stressed under rotating flexure or torsion one can refer to an equivalent diameter d_e obtained taking into account the surface of the section where the tension in higher than the 95% of the maximum tension.
In particular:

$$d_e = \sqrt{\frac{A_{0.95\sigma}}{0,0766}} \quad (24)$$

where:

- $A_{0.95\sigma}$ = surface of the section where the tension $\sigma > 0.95\sigma_{max}$.

In case of axial stress there is no dimensional effect and therefore $k_b=1$ is adopted.

The experimental trials explain that the presence of an indent influences the fatigue duration in a different way in the materials, therefore a concentration factor is introduced for the fatigue tensions K_{tf} calculated in this way:

$$K_{tf} = \frac{\sigma_l}{\sigma_{lt}} \quad (25)$$

where:

- σ_l= fatigue limit of the specimen without indents;
- σ_{lt}= fatigue limits of the specimen with indents

from which the following k_f can be derived:

$$k_f = \frac{1}{K_{tf}} \quad (26)$$

A corrosive environment reduces the fatigue resistance and generally causes the disappearance of the fatigue limit in steels. Moreover the corrosion and the stress exalt to each other deteriorating the behaviour of the material more than the sum of the respective effects.

Fatigue resistance is also influenced by temperature which means that while the high temperature worsens the performances, the low temperature (no matter the more fragile behaviour of the material), improves them. Because of the difficult numerical quantification the coefficient k_e is conglobated into the other coefficient.

EXTENSION OF WOEHLER THEORY TO RAILS

In the following paragraphs the Authors describe the contribution of the extension of the theory of Woehler to the specific case of rails. These elements are subjected to load and unload cycles with a variable amplitude produced by both the passage of trains and by daily thermal excursions.

Woehler curve for thermal stresses

In this case there is no rotating flexure, as it happens in the fatigue tests examined in the general theory, but there is a normal stress alternated with a uniform distribution of tensions in the section. For the construction of the Woehler curve it is assumed a value of σ_R^* equal to [14]:

$$\sigma_R^* = 0,75 \cdot \sigma_R \quad (27)$$

where:

- σ_R^* = cracking stress after axial stress (superior limit of the field of the time limit resistance);
- σ_R = characteristic rupture stress of the material.

The basic fatigue limit, in case of traction or compression without eccentricity, is equal to 45% of the material resistance obtained from the traction test, or:

$$\sigma_{a\infty} = 0,45 \cdot \sigma_R \quad (28)$$

The limit found in this way refers to a standardised specimen, and therefore if one wanted to move to the effective value of the rail σ_l, he should apply the (22) which, neglecting the coefficient k_e, and from a distance away enough from the holes of the head (k_f=1), assumes the following form:

$$\sigma_l = k_a \cdot k_b \cdot k_c \cdot \sigma_{a\infty} \quad (29)$$

with obvious meaning of the terms.

Considering that:

- the rail is obtained from hot lamination (a=57,7 e b=-0,718 – Cfr. Tab. 2);
- the stress is axial (K_b=1);
- the exercise stress is surely lower than 1520MPa (kc=0,850 – Cr. Tab. 1)

the expression (29), respecting (28), assumes the following form:

$$\sigma_l = 22,07 \cdot \sigma_R^{0,282} \quad (30)$$

The equation of the Woehler curve in the bi-logarithmic plane, passing through the points S and G with Cartesian coordinates $(10^3, \sigma_R^*)$ and $(2 \cdot 10^6, \sigma_l)$, gives the following result:

$$N = 10^3 \cdot \left(\frac{\sigma}{\sigma_R^*} \right)^k \qquad \text{per } 10^3 < N < 2 \cdot 10^6 \tag{31}$$

where:

$$k = \frac{\log(2 \cdot 10^3)}{\log \frac{\sigma_l}{\sigma_R^*}} \tag{32}$$

In the remaining variation range on N the Woehler curve of the rail subjected to the only thermal stresses is described indeed by the following laws:

- $\sigma = \sigma_R^*$ per $N < 10^3$; (33)
- $\sigma = \sigma_l$ per $N > 2 \cdot 10^6$. (34)

Woehler curve for stresses due to moving loads

The stress produced in the rail after the moving loads transit is mainly flexural and the maximum value is reached in correspondence of the extreme fibres of the transversal fibres locate at the maximum distance from the neutral axle.

For the construction of the Woehler curve it is assumed a value of σ_R^* equal to [14]:

$$\sigma_R^* = 0{,}9 \cdot \sigma_R \tag{35}$$

where:

- σ_R^* = cracking stress for flexural stress;
- σ_R = cracking stress typical for the material.

The fatigue limit $\sigma_{a\infty}$ refers to a standardised specimen for which, passing from the effective value of the track, it was followed the same pattern of the case analysed in the previous paragraph (Cfr Eq. 29)

The basic fatigue limit, in case of alternated flexure, is equal to 50% of the material resistance obtained from the tensile test, or:

$$\sigma_{a\infty} = 0{,}50 \cdot \sigma_R \tag{36}$$

Since the track is obtained by hot lamination, for the corrective factor k_a the same consideration of the previous paragraph can be assumed, while for the coefficient k_c it is assumed (Cfr. Tab. 1):

$$k_c = 1{,}0 \tag{37}$$

For the calculation of k_b one should evaluate the equivalent diameter (Cfr. Eq. 24) considering that, in the specific case the area $A_{0.95\sigma}$ is delimitated by the upper part of the track fungus and by a chord located at a certain distance x from the neutral axle. In particular, calling with h the height of the rail (in mm) and with y_g the location of the neutral axle with respect to the base of the section (in mm), it can be written:

$$x = 0{,}95 \cdot (h - y_g) \tag{38}$$

One should notice that the section characterised by the $A_{0.95\sigma}$ is a rectangle with rounded off corners; for the sake of computational simplicity and without determining significant variations on the value of k_b it is possible to assimilate this section to a rectangle with a height equal to x and base b equal to the width of the track fungus (b=70mm for the 50 UNI rail and b=74,3mm for the 60 UIC rail). As a consequence:

$$A_{0,95\sigma} = b \cdot (h - y_g - x) \tag{39}$$

At this point, known the geometrical characteristics of the rails and applying the (38) and (39) it is possible to derive the value of d_e (Cfr. Eq. 24):

- d_e = 57,27mm 50 UNI rail
- d_e = 62,66mm 60 UIC rail

Since 50mm ≤ d_e ≤ 100mm it means that (Cfr. Tab. 3):

$$k_b = 0{,}6 \div 0{,}75 \tag{40}$$

and therefore the fatigue limit of the rail for variable loads is:

$$\sigma_l = 57{,}7 \cdot \sigma_R^{-0{,}718} \cdot 1 \cdot k_b \cdot 0{,}50 \cdot \sigma_R \tag{41}$$

It is thus possible to say that the Woehler curve for a rail subjected to the sole stresses due to moving loads is described by the same law found in the previous paragraph (Cfr. Eq. 31÷34), but applying to it the expressions (35, 36, 40, 41).

FATIGUE VERIFICATION

Mechanical elements are often subjected to load histories characterised by variable amplitude cycles (example n_1 cycles with alternated tension σ_1, n_2 cycles at σ_2 and so on).
A simple ad reliable analysis describing the phenomenon of fatigue is represented by the theory of Palmgreen-Miner, according to which every load cycle produces a partial damage and the sum of these damages determinates the rupture. In this way the damage D caused by n cycles with amplitude $\sigma>\sigma_{a\infty}$ is defined as:

$$D = \frac{n(\sigma)}{N(\sigma)} \tag{42}$$

where $n(\sigma)$ is the number of cycles with amplitude σ at which the specimen was subjected and $N(\sigma)$ the number of cycles that brings to the specimen cracking in correspondence of the tension σ.
In the specific it could result D=0 (no damage), D=1 (failure), D<1 (partial damage).
Indicating with D_1 the damage after n_1 cycles with amplitude σ, with D_2 the damage which can still be caused and with n_2 cycles of the same stress amplitude, before getting to failure, the expression $D_1+D_2=1$ individuates the rupture condition for a number of cycles equal to $N=n_1+n_2$.
Generalising these observations the linear accumulation of the damage theory can be found, which was proposed by Miner in 1945, which says: "*the accumulated damage at every level of amplitude of stress σ_i so that $\sigma>\sigma_{a\infty}$ reflects itself on the life of the piece for each tension applied and the rupture will be reached when the sum of the damages is equal to one*".
This hypothesis can be extended to a larger number of load cycles with different amplitude and in this case the rupture conditions becomes:

$$D = \sum_i \frac{n_i(\sigma_i)}{N_i(\sigma_i)} = 1 \tag{43}$$

with the following meaning of the symbols:

- $n_i(\sigma_i)$ = number of effective cycles relative to every amplitude level present;
- $N_i(\sigma_i)$ = number of cycles for rupture in correspondence of σ_i.

The contribution of the Authors in this paper is concentrated on the definition of an operative procedure able to connect Miner's law to the theory of Woehler for the fatigue analysis in the long welded rail.

Fatigue verification of the rail for thermal stresses

Because of thermal gradients axial stresses arise in the rail, which cyclically vary from a minimum to a maximum daily value. Therefore the rail is daily subjected to a not constant amplitude load cycle.
The presence of an effective number of cycles allows the application of Miner's law and of the Woehler's theory. More specifically the following operations are to be followed:

1) assignment of daily minimum and maximum temperatures ($t_{min,i}$ and $t_{max,i}$);
2) calculation of the thermal stress σ_i through the following formula:
$$\sigma_i = 237 \cdot A \cdot (t_{\max,i} - t_{\min,i}) \tag{44}$$
with obvious meaning of the symbols.
3) counting of the effective cycles n_i for each stress σ_i;
4) calculation of the number N_i of rupture cycles in correspondence of each stress σ_i (Cfr. Eq.31, 33 and 34);
5) calculation of damage according to Miner's theory with the following formula:
$$D = \sum_i \frac{n_i(\sigma_i)}{N_i(\sigma_i)} \tag{45}$$
6) analysis of the obtained damage (if D<1 the verification is satisfied and the rail can bear further variations of temperature, while if D>1 the rail gets to fatigue cracking).

Fatigue verification of the rail after loads stresses

The stresses on the rail because of the presence of running loads can assume different values, the section and the class of steel being the sale, as function of the axle weight of the train.
They alternate cyclically with time as function of the exercise conditions of the track line, therefore also in this case the rail fatigue verification is fundamental.
Referring to the thousands of cycles acting on the rail, there are some cycles labelled with a stress σ_i and a parameter n_i corresponding to the number of passages, in the verification period, of the axle with weight P_i

which determinates the σ_i. The calculation of the stresses due to the passage of an axle of weight P made through the theory of Timoschenko (continuous beam on discontinuous supports resting on a Winkler elastic soil), gives the following equation:

$$\sigma = \frac{C_d}{W} \cdot \frac{P \cdot L_v}{8} \tag{46}$$

where:

- C_d = coefficient of dynamic increment(1);
- W = resistance modulus of the section in cm^3;
- P = weight per axle in t;
- L_v = wave length (in cm) of the elastic line because of the presence of an isolated load.

In particular, labelling with E the modulus of longitudinal elasticity of steel expressed in N/cm^2, with J the modulus of inertia in cm^4 of the rail with respect to the centre of gravity axle and with k an appropriate parameter expressed in N/cm^2, the result is:

$$L_v = \sqrt[4]{\frac{4 \cdot E \cdot J}{k}} \tag{47}$$

where:

- $k = \frac{k_v \cdot S}{I_t} = \frac{k_v \cdot (b \cdot u)}{I_t}$ (48)
- k_v = subgrade modulus(2);
- S = effective support surface of the sleeper in correspondence of each rail in cm^2;
- I_t = span of sleepers in cm;
- b = sleeper width in cm;
- u = length of the part of the sleeper involved in the loads distribution generated by the rail.

The operative phases of the fatigue verification of the rail after the application of the running loads, are therefore the following:

1) calculation for each typology of axle P_i of the corresponding stress σ_i (Cfr. Eq. 46);
2) counting of the number n_i of passages for each type of axle "i" (product of the number of daily passages multiplied by the verification days). In order to take into account the evolution of traffic with time it is important to introduce the annual traffic increment rate r_i, specific for each axle, and calculate the overall number of passages after a number of years equal to the verification period, applying the following relation:

$$n_i^* = n_i \cdot \sum_{j=1}^{m} \left(1 + r_i\right)^{j-1} \tag{49}$$

where:

n_i^* = overall passages of the axle "i" at the end of the verification period;

n_i = annual passages of the axle "i" at the actuality;

m = verification period in years;

r_i = annual traffic incremental rate relative to the axle "i";

3) calculation of the number N_i of rupture cycles in correspondence of each stress σ_i (Woehler curve for stresses due to moving loads);
4) damage calculation according to Miner's theory.
5) analysis of the obtained damage.

Therefore the verification keeps going analysing the total damage obtained summing the damage induced by thermal stresses and that induced by loads; if the total damage (Cfr Eq. 43) is smaller that 1 the verification is satisfied, while if it is bigger or equal to 1 the rail is to be changed.

CONTROLS OF THW LWR IN EXERCISE

Ferrovie dello Stato, according to what established in [11], periodically checks the thermal asset of the rail measuring the clearance. This measurement, made in spring and in presence of high or low temperatures, involves the recording of the data on specific prospects on respectively the body and the edges of the LWR and includes the reading, by means of graduated identification tags, of the existing clearance between the junctions and the displacements of the reference points at the edges of the rail.

From the analysis of the data some situations were found where the differences between the values of the effective clearances and of the theoretical clearances needed maintenance interventions (clearances corrections, regularization of clearances, regulation of internal tensions).
Moreover, through the analysis of the diagrams of the stresses in the body and at the edge of the LWR, it is possible to find the presence of excessive tensions which stress the rail.
In order to shorten the analysis times of the thermal asset of the track and to automate the applicative part of the Woehler's curve construction, the calculation of the internal stresses and the calculation of the damage according to Miner's law, the Authors arranged a dedicated software called THERMICRAIL, described in the following paragraph.

THERMICRAIL CALCULATION CODE

The THERMICRAIL calculation code, realised in Visual Basic 6.0®, allows the execution of the fatigue thermal analysis of the LWR. In particular the fatigue verification is divided in two phases:
1) thermal stresses verification;
2) overall verification for thermal stresses and stresses due to running loads.

The analysis of the thermal asset needs the insertion of the following input data (Cfr. Fig. 8):
- rail type (50 UIC or 60 UIC);
- sleepers material (wood or prestressed concrete);
- maximum and minimum daily temperature.

On the basis of these data the code gives the regulation temperature, the temperature of opening and total closure time of clearances and elaborates the following diagrams:
- complete hysteresis cycle of clearances (Cfr. Fig. 9);
- diagram of the forces in the body of the LWR (Cfr. Fig. 10);
- diagram of the forces at the edges of the LWR (Cfr. Fig. 11).

As already noted, the code allows the recording of the data relative to the controls in use in the body and at the edges of the LWR, automatically reproducing the prospects used by Ferrovie dello Stato.
The study of the fatigue phenomenon was implemented referring to the Woehler's theory (construction of the curves stress÷number of cycles) and to Miner's linear accumulation law (real verification).
THERMICRAIL executes automatically all the applicative part on the Woehler's curve, the calculation of the internal stresses and the calculation of the damage according to Miner's law, asking for the following data as input (Cfr. Fig. 12):
- class of rail steel;
- length (in year) of the period of verification;
- extreme daily temperature values in the verification period.

For the complete verification which considers simultaneously the effects of thermal stresses and of the load stresses, it is necessary to include further data in the second section of the dialog box.
First of all it is necessary to chose, from the top to the bottom, the following:
- kind of rail between the two options 50 UNI and 60 UIC;
- the sleepers width in cm;
- the modulus or the span of sleepers in cm;
- the length of the support area of the sleepers in cm;
- the subgrade constant in kg/cm^3.
-

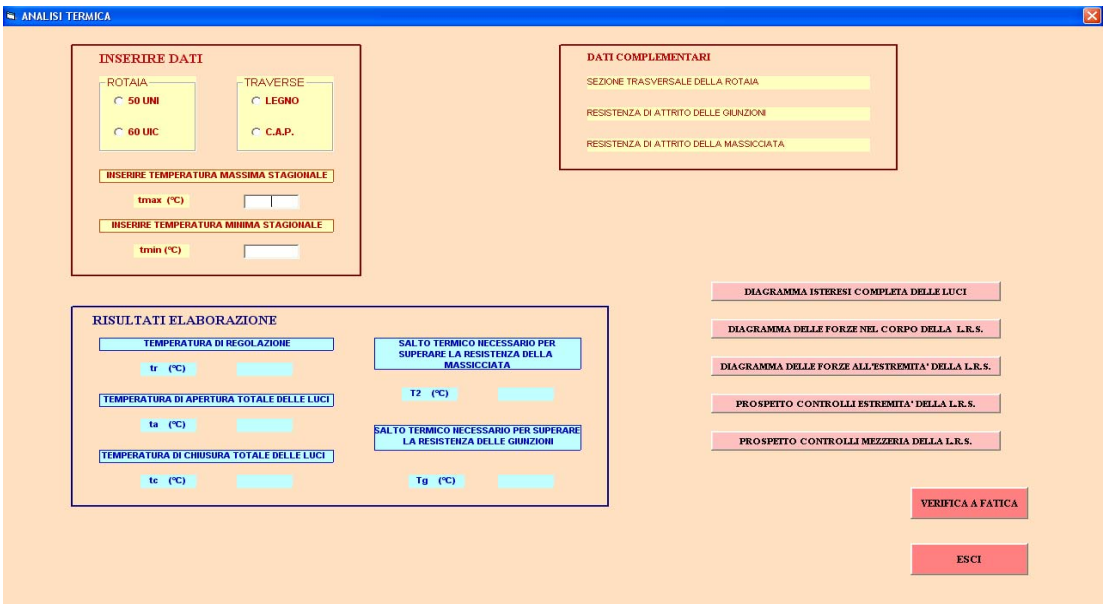

Figure 8: "Thermal analysis" window

After that it is necessary to include the data in the running loads on the rail (number of axles, annual increase rate and weight). For the recording of these values the following steps are needed:

- digit the weight of the axle in t, in the homonymous box;
- digit the number of daily passages in the relative box;
- digit the annual increase rate of traffic, r, relative to the axle just inserted.

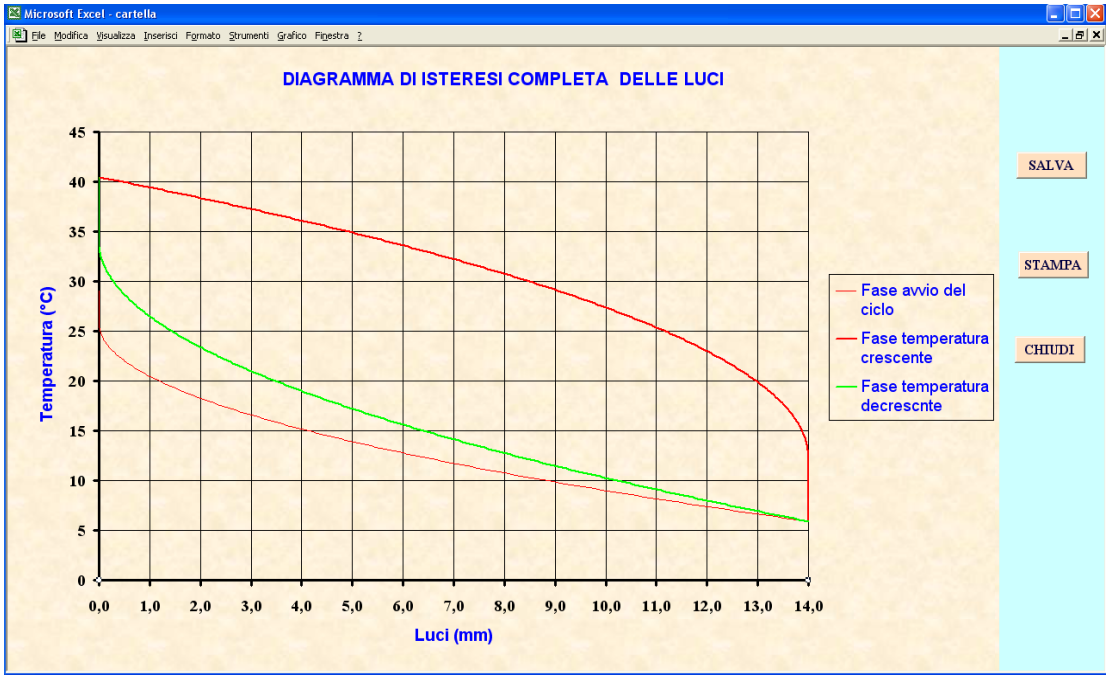

Figure 9: "Hysteresis diagram with spans" window

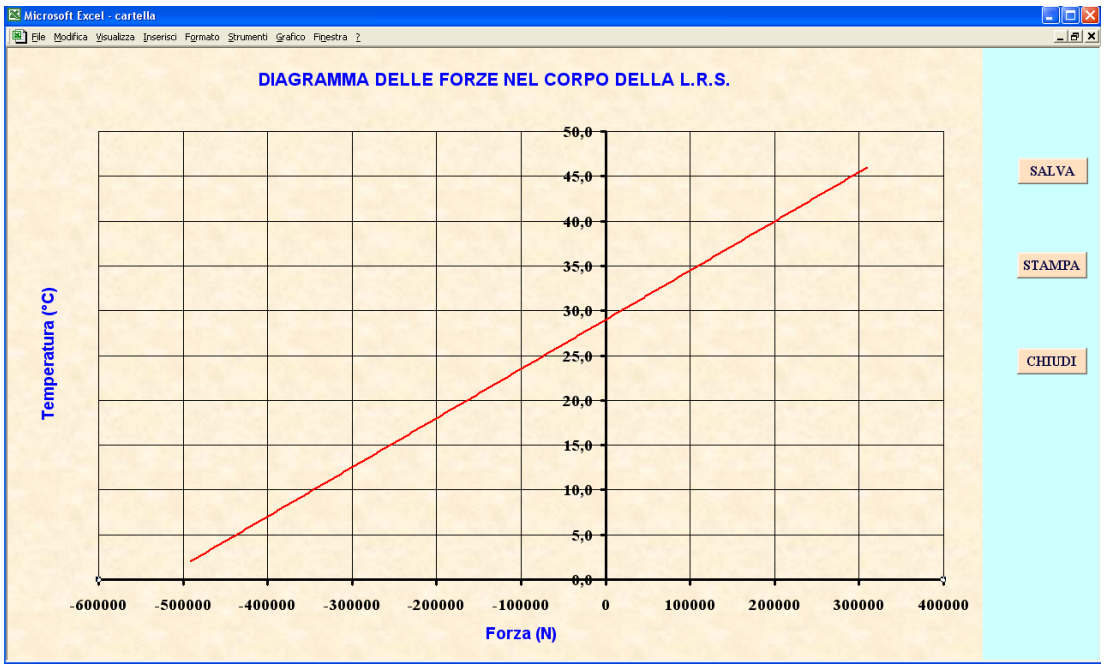

Figure 10: "Forces diagram in the body of the LWR" window

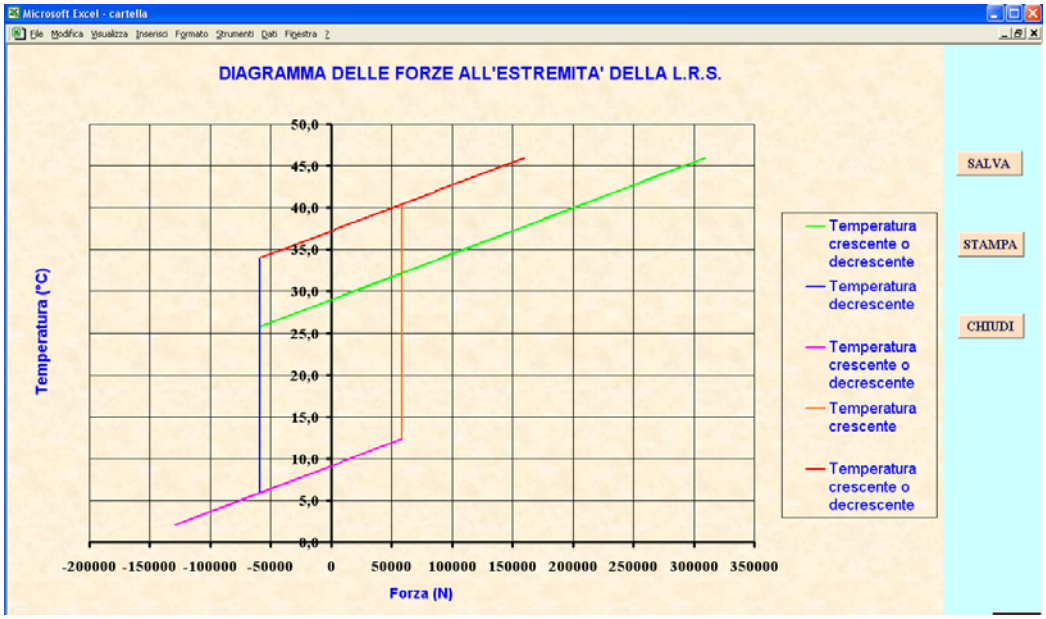

Figure 11: "Forces diagram at the edge of the LWR" window

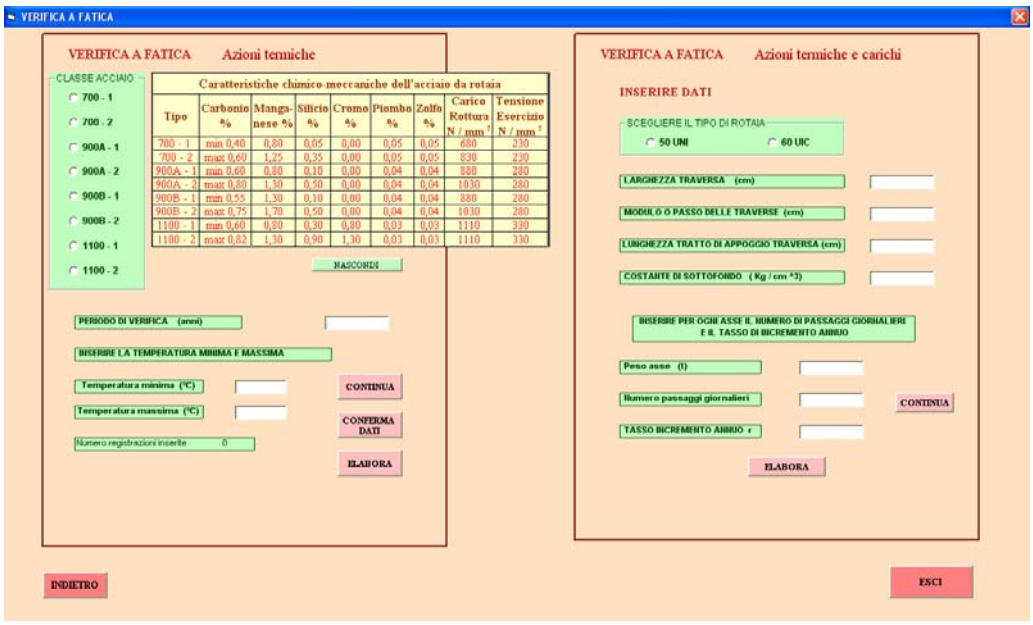

Figure 12: "Fatigue verification" window

For a higher clarity here is the flow diagram of the calculation code (Cfr. Fig. 13).

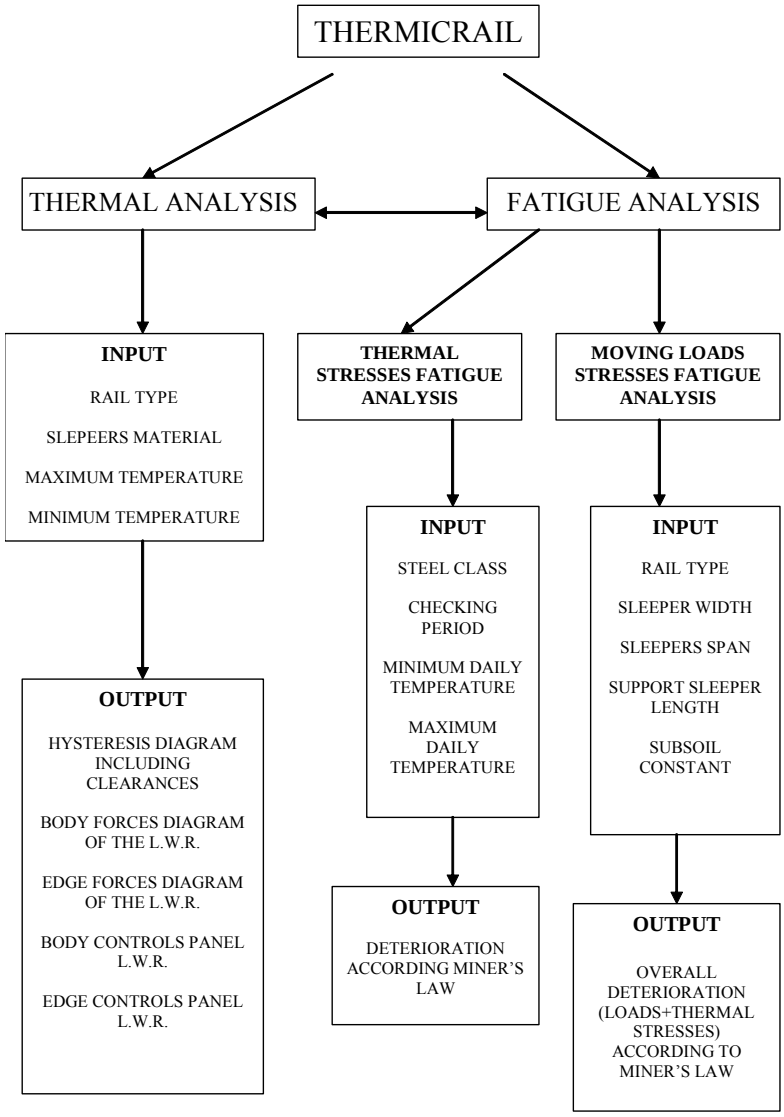

Figure 13: THERMICRAIL code flow diagram

CONCLUSIONS

The thermal analysis of the LWR highlighted the existence of a cyclic stress phenomenon, characterised by the alternation of maximum and minimum values, so that the fatigue verification after thermal stresses is surely very interesting.
The study of fatigue was conducted by the Authors referring to both Winkler's theory, for the construction of the curves stress÷number of cycles and Miner's law of linear accumulation, for the real verification.
Starting from the consideration that thermal variations generate in the rail uniformly distributed axial tensions, it was necessary to arrange the specific Woheler curve for the rail, considering the experimental indications and appropriate coefficients, so that afterwards the calculation of the linear damage was possible.
For a complete analysis the effect of continuous and repeated passage with time of moving loads was also taken into account.
From an operative point of view the fatigue verification for thermal stresses was performed in the same way. In particular, once the new Woehler curve was constructed, for each axle typology the induced stress and the number of repetitions during the verification period were assessed.
Applying Miner's theory not only the damage due to daily thermal excursions was calculated, but also the overall damage by both thermal stresses and moving loads.
A further contribution was given by the Authors through the arrangement of the so-called THERMICRAIL calculation code, prepared in visual Basic 6.0®, which automatically executes all the applicative part on the construction of the curve of Woehler, the calculation of internal stresses and the calculation of damage referring to Miner's law, allowing in this way the strong reduction of analysis times.
Therefore, THERMICRAIL is a valid instrument which allows the monitoring of the stress state of the rail and to study the case where possible structural collapse could happen.
This code, apart from giving an exhaustive analysis of the thermal asset of the LWR and from allowing an appropriate maintenance interventions planning, allows a detailed fatigue verification in order to optimise the life cycle of the track.
In conclusion, the positive outcomes with the theoretical-experimental experiences conducted so far give credit to a possible diffused and reliable use of the proposed methodology.

ENDNOTES

(1) Different formulations of the coefficient C_d were given as function of velocity. Ferrovie dello Stato use instead values which are independent to the velocity and are:
- 1,75 traditional track in regular use conditions;
- 3,60 traditional track in exceptional use conditions;
- 1,50 track without ballast in regular use conditions;
- 2,50 traditional track in exceptional use conditions.

(2) The subgrade coefficient K_v is defined as the pressure under the sleeper which causes a unitary lowering. In particular it assumes the following values:
- $k_v = 20 \div 30$ N/cm^3 poor subgrade;
- $k_v = 50 \div 90$ N/cm^3 medium subgrade;
- $k_v = 100 \div 180$ N/cm^3 good subgrade.

REFERENCES

[1] MINISTERO DEI TRASPORTI FERROVIE DELLO STATO–SERVIZIO LAVORI E COSTRUZIONI (1959), *Istruzioni sulle luci di dilatazione delle rotaie*, Circolare N°61 del 24/06/1959.
[2] MINISTERO DEI TRASPORTI FERROVIE DELLO STATO–SERVIZIO LAVORI E COSTRUZIONI (1959), *Esecuzione dei lavori di manutenzione in corrispondenza dei binari con rotaie di lunghezze normali e con lunghezze saldate (l.r.s.)*, Circolare N°63 del 27/06/1959.
[3] MINISTERO DEI TRASPORTI FERROVIE DELLO STATO–SERVIZIO LAVORI E COSTRUZIONI (1959), *Lavori di ricostruzione della massicciata*, Circolare N°69 del 03/08/1959.
[4] MINISTERO DEI TRASPORTI FERROVIE DELLO STATO–SERVIZIO LAVORI E COSTRUZIONI (1959), *Lavori all'armamento*, Circolare N°114 del 19/12/1959.
[5] ANGELERI G. (1969), *Termica del binario*.

[6] ANGELERI G., FOCACCI C., GADDINI C., GENNARI G., TRETENE F. (1976), *Manuale tecnico del binario 8 – Lavori al binario*, Vol. 1 e 2 , Scuola Centrale del Servizio Lavori e Costruzioni delle F.S.
[7] LANNI S. (1979), *La termica del binario*, CIFI Collana di testi per la formazione e l'aggiornamento professionale.
[8] ENTE FERROVIE DELLO STATO–SERVIZIO LAVORI E COSTRUZIONI (1987), *Sicurezza nei confronti dello svio*; *valori limiti dello sghembo del binario* , Circolare L.41/344/7.9 del 28/09/87.
[9] MAYER L. (1989), *Impianti ferroviari – Tecnica ed esercizio*, CIFI – Collegio Ingegneri ferroviari Italiani, Roma.
[10] Tesoriere G., *Strade Ferrovie Aeroporti* (1990), Vol. 1 e 2, UTET, Torino.
[11] FERROVIE DELLO STATO (1990), *Istruzione sulla costituzione ed il controllo delle l.r.s.*, Istruzione del 19/11/1990.
[12] DIRETTIVA CEE (1991), 440/91.
[13] CORVINO L. (1993), *Manuale del tecnico del binario – La costituzione il controllo e la manutenzione delle lunghe rotaie saldate*, vol. 5, Collegio Ingegneri Ferroviari Italiani, Collana di testi di cultura professionale.
[14] JUNIVALL R. C., MORSHEK K. M. (1994), *Fondamenti della progettazione dei componenti delle macchine*, Edizioni ETS.
[15] CORVINO L. (1994), *Manuale del tecnico del binario – La termica del binario*, vol. 7, Collegio Ingegneri Ferroviari Italiani, Collana di testi di cultura professionale.
[16] BONO G., FOCACCI C., LANNI S. (1997), *La sovrastruttura ferroviaria*, Collegio Ingegneri Ferroviari Italiani, Collana di testi di cultura professionale.
[17] ATZORI B. (2000), *Appunti di Costruzione di macchine*, Edizioni Bibreria Cortina, Padova.
[18] TELLARINI G. (2000), *Programmazione generale e regolazione specifica del settore trasporto ferroviario alla luce del nuovo piano generale dei trasporti* - Università di Bologna, Convegno del 15/11/2000 di Manutenzione nei trasporti ferroviari, Associazione Italiana di Manutenzione (AIMAN).
[19] GALFRÈ M., NACHERIO L. (2000), *Esempi di attrezzature (on train e off train) per il monitoraggio periodico delle caratteristiche di qualità di marcia del rotabile*, Fiat Industrie Ferroviarie, Convegno del 15/11/2000 di Manutenzione nei trasporti ferroviari, Associazione Italiana di Manutenzione (AIMAN).
[20] NAGGAR R. (2000), *Manutenzione ordinaria del binario, chiavi in mano, su linee principali*, ANIAF Bologna, Convegno del 15/11/2000 di Manutenzione nei trasporti ferroviari, Associazione Italiana di Manutenzione (AIMAN).
[21] LUNGHI C. A. (2000), *Esempio di manutenzione di una ferrovia minore: Ferrovia Ferrara Suzzara* Convegno del 15/11/2000 di Manutenzione nei trasporti ferroviari, Associazione Italiana di Manutenzione (AIMAN).
[22] RETE FERROVIARIA ITALIANA, (2001), *Norme tecniche sulla qualità geometrica del binario,* Istruzione tecnica TCAR ST AR 01 001 del 30/11/2001.
[23] BASILE A. (2002), *L'Innovazione Tecnologica nel contesto Ferroviario*, Bollettino della Comunità Scientifica in Australia.